How travertine veins grow from top to bottom and lift the rocks above them: The effect of crystallization force

Jean-Pierre Gratier[1], Emanuelle Frery[1,5], Pierre Deschamps[2,3], Anja Røyne[4], François Renard[1,4], Dag Dysthe[4], Nadine Ellouz-Zimmerman[5], and Bruno Hamelin[2]

[1]ISTerre, University Grenoble 1 & CNRS, BP 53, Grenoble 38041, France
[2]Aix-Marseille Université, CEREGE, UMR 6635, 13545 Aix-en-Provence cedex 4, France
[3]IRD, CEREGE, UMR 161, 13545 Aix-en-Provence cedex 4, France
[4]Physics of Geological Processes, University of Oslo, 0316 Oslo, Norway
[5]IFP Énergies nouvelles, Rueil-Malmaison, 92852, France

ABSTRACT

Travertine mounds form at the mouth of springs where CO_2 degassing drives carbonate precipitation from water flowing from depth. Building of such mounds commonly involves the successive "stratigraphic" deposition of carbonate layers that precipitate from waters rising from depth along vertical to horizontal open fissures that are episodically sealed by radiating crystals. Much more intriguing structures can also be observed, such as widespread horizontal white veins of carbonate with vertical aragonite fibers, parallel or oblique to the "stratigraphic" travertines, which extend laterally over distances of several tens of meters and could represent up to 50% of the total volume of the travertine mound. Using highly precise U-Th dating, the growth direction of these horizontal veins is shown to be from top to bottom, and this fact clearly indicates that they developed within the mound over a period of ~1000 yr for the vein analyzed. A vein growth mechanism is proposed that is able to uplift the rock above the vein thanks to the force of crystallization. The possible development of such structures in other places and the consequences of reverse growth direction when interpreting travertine data are discussed.

INTRODUCTION TO TRAVERTINE GEOLOGY

Travertine mounds are carbonate rocks that form at the mouth of springs where CO_2 degassing drives mineral precipitation from carbonate-supersaturated water flowing from depth. This study concerns thermogenic travertine mounds that grow along the Little Grand Wash and Salt Wash normal faults in central Utah (United States; Fig. 1) and bear witness to the past and present activity of carbonate-rich springs (Dockrill and Shipton, 2010; Kampman et al., 2010). The internal structure of some mounds has been revealed by erosion, providing evidence of the complex processes that occurred at depth. U-Th ages obtained for these carbonates vary from 5 to 135 k.y. (Dockrill, 2006; Kampman et al., 2012). Evidences of flow paths are revealed by the bleaching of the red sandstones below the travertine mounds (Fig. 2A): CO_2-rich fluid flows from depth along normal faults and their associated fracture networks. Figure 2 shows a sketch of four processes involved in the building of these travertine mounds. The best-known process is the successive deposition of carbonate layers that precipitate as a result of degassing of water exiting springs or geysers. These "stratigraphic" travertine layers, with varying dip, develop from bottom to top (Fig. 2B) and are most often mixed with river sand or windblown particles that give them a dark color. Another type of common structure at depth are vertical fissures (Fig. 2C) filled with banded travertine (Hancock et al., 1999). Such structures have been studied in other regions to reconstruct regional tectonic stress variations (Faccenna et al., 2008; Uysal et al., 2007). Most

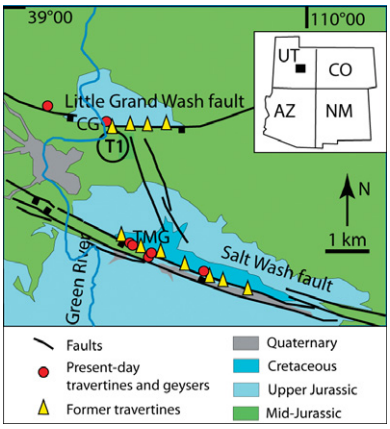

Figure 1. Map of the study area. Location of the Little Grand Wash and Salt Wash faults in the Colorado Plateau (Utah), and simplified geological map with the location of the active geysers with fossil and active travertine deposits, Crystal Geyser (CG) on the Little Grand Wash fault and Ten Mile Geyser (TMG) on the Salt Wash fault. The travertine mound studied is labeled T1. Adapted from Dockrill (2006) and Frery (2012).

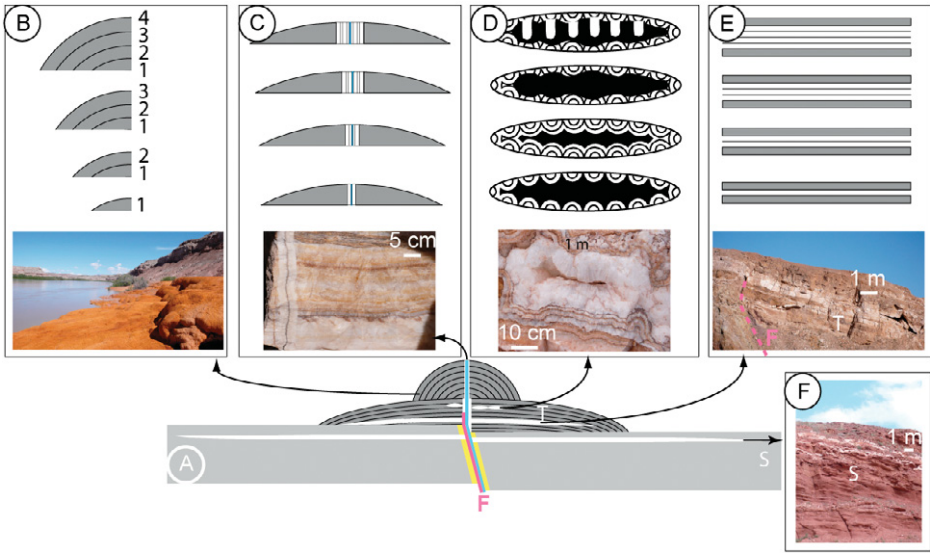

Figure 2. A: Sketch of a cross section of the travertine mound studied, with the various types of deposits (above). Normal fault trace is red, bleaching paths are yellow, and fluid paths are blue. T—travertine mound; F—fault; S—sandstone. B: "Stratigraphic" surface travertine with bottom-to-top growth. C: Vertical fissure travertine with more or less symmetric banded growth from the vein-rock contact to center of the vein. D: Open self-supported cavities partially sealed with radiating carbonate crystals with evidence of dissolution and redeposition (as stalactite-like structure). E: Horizontal white veins with incremental episodes of growth in the travertine mounds (T). F: Horizontal white veins extending laterally over large distances (hundreds of meters) in the surrounding sandstones (S).

GEOLOGY, November 2012; v. 40; no. 11; p. 1015–1018 | doi:10.1130/G33286.1 | Published online 22 August 2012

often, in fissure travertine of this type, crystals can be observed to have grown from the vein-rock contact to the center of the vein, more or less symmetrically (Fig. 2C). Connected to such conduits are typical open vertical to horizontal cavities partially sealed with radiating acicular calcite or aragonite crystals. Paired banded layers and bumpy surfaces face each other toward the center of the cavity (Fig. 2D) (Shipton et al., 2004). Evidence of dissolution or redeposition, such as stalactite-like structures (Fig. 2D), reflect the permanent opening of such cavities with either deposition, or dissolution, or successively both, depending on the degree of saturation of the fluid. These three types of structures are commonly described in travertine mounds (Pentecost, 2005).

Much more intriguing structures are observed, such as the widespread horizontal white veins of pure carbonate that are oriented parallel or obliquely to the stratigraphic darker travertines, with vertical fibers (Fig. 2E). The thickness of the veins varies from a few centimeters to tens of centimeters. These veins extend laterally over distances of several tens of meters and represent up to 50% of the total volume of the travertine mound (Fig. 3A). Such horizontal veins are also observed in the sandstone basement, away from the travertine but near the surface at less than 10 m depth (Fig. 2F) and always in the vicinity of arrays of bleached paths connected to the normal faults (Fig. 2A). These horizontal veins raise several questions: Do they develop at the surface in continuity with the stratigraphic travertine or are they internal structures that develop within the mound after it has been built? And in this latter case, what could be the growth mechanism since it must lead to uplifting of the rock above the vein (Fig. 2E)?

STUDY OF HORIZONTAL TRAVERTINE VEINS

We investigated one of these horizontal veins, 27 cm thick, located in a travertine mound near the Crystal Geyser along the Little Grand Wash (arrow, Fig. 3A). Both microstructural observations of the successive layers and U-Th dating were performed on four carbonate samples collected perpendicular to the growth banding (see Fig. 3B).

U-Th Dating

Samples of 2–3 g of pure aragonite were spiked with mixed ^{236}U-^{233}U-^{229}Th and dissolved in nitric acid before separating the U and Th fractions using standard techniques. U-Th measurements were performed by thermal ionization mass spectrometry (TIMS) using a VG-Sector 54-30 mass spectrometer (Deschamps et al., 2012). Very high ^{238}U concentrations (7.2–9.2 ppm) combined with high $^{234}U/^{238}U$ ratios and low detrital ^{232}Th concentrations result in U-Th age uncertainties of 0.15%–0.2% (2σ). Initial ratios, $(^{234}U/^{238}U)_0$, are relatively constant, ranging between 4.19 and 4.26, and reflect the broad constancy of the fluid composition.

The four dating results indicate a vein growth from top to bottom: the youngest layer (5851 ± 10 yr) lies at the bottom of the travertine whereas the oldest (6830 ± 14 yr) is located at the top. Two intermediate samples were dated at 5922 ± 9 yr and 6355 ± 11 yr. The total vein building duration was ~1000 yr over the 270 mm width, with a mean growth rate of 0.27 mm/yr. Note also that the growth rate varied from 0.2 to 0.92 mm/yr (Fig. 3B).

Microstructural Analysis

Structural and microstructural observations show both the general continuity of the growth of aragonite fibers and some slight heterogeneity of the crystallization process at various scales. Veins banding with slight differences of color are seen at the decimeter scale (Fig. 3B), but do not show any clear correlation with stable isotope composition evolution (Frery, 2012). Near-horizontal parallel-to-the-vein undulating surfaces at the centimeter (Fig. 3C) to millimeter scale (Fig. 3D) are locally correlated to slight changes in aragonite fiber growth direction and locally mark the site of aragonite replacement by calcite (Fig. 3D). However, some aragonite fibers crosscut in continuity through these surfaces. Fan-shaped fibers of both aragonite and calcite indicate the growth direction, from top to bottom. Arrays of vertical fractures and vertically elongated pores between the fibers are often rooted on subhorizontal surfaces (Figs. 3E–3G). At a smaller scale, the development of horizontal stylolites (Fig. 3H) indicates a vertical compressive stress. Altogether, these observations point to a near-continuous growth of the aragonite fibers, from top to bottom, through the full width of the veins.

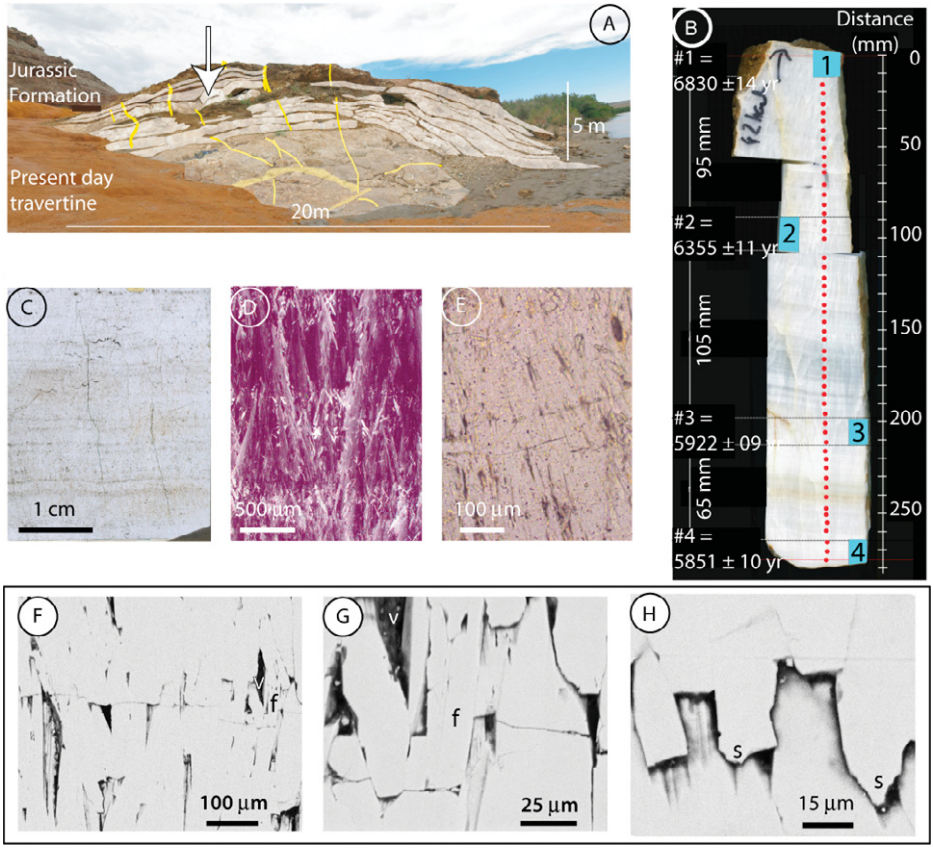

Figure 3. A: Horizontal white veins in eroded travertine T1 (see Fig. 1) with the dated vein (arrow). Horizontal veins are highlighted in white; vertical veins in yellow. B: U-Th ages for four samples. Results range from 6830 to 5851 yr, and indicate a top-to-bottom growth direction. Red points indicate location of samples for chemical analysis (Frery, 2012). C,D: Near-horizontal parallel-to-the-vein surfaces at centimeter (C) to millimeter scale (D) are correlated to some slight changes in the direction of the aragonite fibers (D), where a fan-shaped fiber structure can be seen to have nucleated at the same horizontal location. E–G: Arrays of vertical fractures and vertically elongated pores (v) between fibers (f) rooted on subhorizontal surfaces. H: Horizontal stylolite (s) indicating vertical compressive stress.

DISCUSSION AND CONCLUSIONS

The first question to be asked is how can precipitation lead to an uplift of the rock above the vein. It may be considered that an increase in fluid pressure up to the lithostatic value could open such horizontal veins. However, carbonate

precipitation requires a decrease in fluid pressure, so it would have to be assumed that the growth rate is faster than the rock collapse rate when the fluid pressure decreases, which is not realistic for veins of such lateral extent. An alternative explanation is that such veins, growing against gravity, are linked to the force of crystallization (Weyl, 1959), as suggested by several authors to explain the growth of some particular veins (Fletcher and Merino, 2001; Hilgers and Urai, 2005; Wiltschko and Morse, 2001). It has also been shown experimentally that mineral precipitation can uplift a dead weight (Taber, 1916) and can induce intense fracturing (Noiriel et al., 2010). From equilibrium thermodynamic considerations, it is found that a crystal face subjected to a differential pressure ΔP (the difference between the surface normal stress and the pore fluid pressure) is in equilibrium with a solution of supersaturation ratio Ω, defined as the ratio between the ion activity product in solution and the solubility product of the solid, through the following relation (Steiger, 2005):

$$\Delta P = \left(RT/V_s\right)\ln\Omega, \qquad (1)$$

where R is the gas constant, T is the temperature (K), and V_s is the molar volume of the solid. In this example of a horizontal vein, with top-to-bottom growth direction, precipitation takes place at the lower vein-rock contact (Fig. 2E), in the thin fluid phase with supersaturation ratio Ω, which is trapped along the vein seam, and uplifts the rock above the vein if ΔP is greater than the lithostatic pressure caused by the weight of the rock column above the vein. Using $V_s = 3.41 \times 10^{-5}$ m^3 mol^{-1}, R = 8.32 m^3 Pa K^{-1} mol^{-1}, T = 291 K, and a stress ranging from 25 to 250 kPa corresponding to the weight of 1–10 m of rock, respectively, the required supersaturation ratio Ω ranges from 1.0008 to 1.008, indicating that a supersaturation level in the range of 0.8–8 per mil is sufficient to uplift the observed mass of rock.

The veins have probably grown at much higher supersaturation levels than this value. At the low temperature and magnesium concentrations found in this system (Heath, 2004; Kampman et al., 2009), the presence of aragonite, a metastable phase, indicates that the fluid may have experienced a large, sudden increase in supersaturation. For example, aragonite forms in surface travertine deposits when the rate of CO_2 degassing is sufficiently high (Pentecost, 2005). Chemical analyses from nearby springs (Heath, 2004; Kampman et al., 2009) also show that the fluid supersaturation ratio is much greater than that required for the observed uplift: the value of Ω calculated for aragonite is ~1.82 for the Crystal Geyser, and it varies from 1.12 to 4.9 for various geysers and bubbling springs in the region (Fig. 1).

Both observations and chemical data suggest that the veins form when the carbonate saturation increases suddenly at depth. This is most likely caused by CO_2 degassing. Chemical data from nearby springs (Heath, 2004; Kampman et al., 2009) show that fluids in this system have very high concentrations of dissolved CO_2: the partial pressure of gaseous CO_2 in equilibrium with the fluids sampled at the surface is pCO_2 = 100 kPa in the neighboring active Crystal Geyser, and ranges from 50 to 150 kPa in the region. For comparison, pCO_2 in dry air at 1 atm is only ~35 Pa, which means that these fluids are highly supersaturated compared to gaseous CO_2. The solubility of CO_2 increases with depth as fluid pressure increases, so that fluids at large depths are in equilibrium with carbonates. At some critical depth, fluids become metastable with respect to the formation of CO_2 bubbles (Fig. 4A, left). However, if the fluid is confined inside small pores, bubbles will not nucleate before a very high supersaturation level is reached (Or and Tuller, 2002). The isotopic compositions of gases and fluids erupting from the active Crystal Geyser were used by Assayag et al. (2009) to calculate the depth of bubble formation. They found that bubbles must have formed at a depth of less than 100 m. However, the Crystal Geyser was formed in the borehole of an abandoned oil exploration well, and it can therefore be expected that fluids will be largely unconfined in at least the upper 200 m. Conversely, in the context of the travertine veins, fluids are confined at depth in very small pores, which would be expected to suppress bubble formation quite considerably (Oldenburg and Lewicki, 2006). It is therefore likely that CO_2 degassing has taken place in the upper 1–10 m, where the veins have been observed to form. Very high CO_2 concentrations raise the carbonate solubility, producing a high calcium concentration in the pore fluid. When CO_2 ebullition occurs, the fluid suddenly becomes highly supersaturated with carbonate, triggering aragonite formation and vein development at the point where the CO_2 gas is released (see Fig. 4A, right). The progressive development of the veins may be compared to the formation of a subhorizontal ice lens in a temperature gradient (Style et al., 2011): assuming that there is some initial crack porosity in the rock, crystal growth in a small crack could cause it to extend subhorizontally and form a vein at the near-horizontal level of the CO_2 degassing.

A kinetics approach is needed in order to integrate the rate of mass transfer added to the vein. Diffusion in a stagnant fluid cannot produce the fast growth rates observed unless the fluid concentration (of dissolved calcium) is on the order of 1 M, which is unrealistic when comparing with the actual Ca concentration measured in neighboring geysers and springs, which ranges from 7 to 192 mM (Heath, 2004; Kampman et al., 2009). This means that precipitated material must have been supplied to the growing vein by fluid flow (Fig. 4B). If the growth rate $\dot{h}$ of the vein was limited by transport, it would be given by

$$\dot{h} = V_s\left(C_\infty - C_v\right)Q, \qquad (2)$$

where C_v is the equilibrium molar concentration of Ca at the base of the vein, C_∞ is the concentration of Ca at depth, and Q is the volume flux. To test the hypothesis, it was assumed that Q is compatible with a typical desert evaporation rate of 10 m/yr, with the idea that all the water that percolates through the veins must evaporate when reaching the surface. In order to produce the observed growth rate of 0.27 mm/yr, the value of $C_\infty - C_v$ would need to be 0.8 mM, a value that agrees well with the observed Ca concentrations and required supersaturation.

As demonstrated by the dating results, growth occurs at the base of the vein. It may be considered that most of the excess material

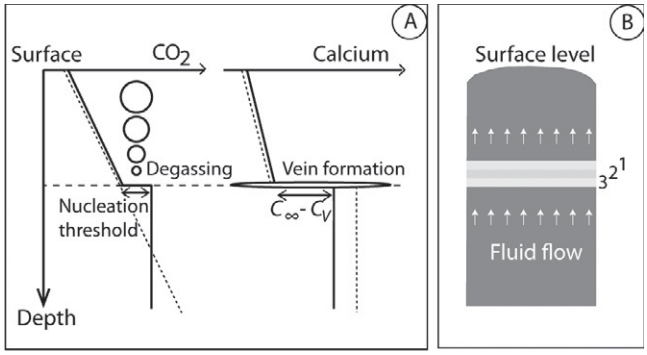

Figure 4. A: Model of carbonate precipitation at depth. Note that slopes and values are only qualitative, for illustration purposes. Dotted lines show equilibrium concentrations. Black lines show fluid concentrations. When fluid concentration is to the left of the dotted line, the fluid is undersaturated; where the two lines cross, the fluid becomes supersaturated. Left-hand side shows how the equilibrium concentration of CO_2 increases with depth: CO_2 concentration is assumed to be nearly constant at depth. At shallow depth, where black line crosses the dotted limit, the fluid becomes metastable with respect to CO_2 degassing. When the supersaturation level is sufficiently high for bubble nucleation, degassing takes place. Right-hand side shows how fluid is initially undersaturated with respect to calcium concentration, which is also assumed to be nearly constant at depth. When CO_2 leaves the system, the equilibrium concentration of calcium decreases dramatically, and aragonite precipitates. The largest volume precipitates at the base of the vein, where the supersaturation is highest. B: Growth of carbonate crystals with top-to-bottom growth direction resulting from the carbonate crystallization force triggered by CO_2 degassing at shallow depth.

is consumed there and that the fluid flowing through the veins is close to equilibrium with the carbonate in the vein. Observed local calcite growth, at the expense of the initial aragonite fibers (Fig. 3E), may be an effect of such fluid flow through the veins: it has been shown (Perdikouri et al., 2008) that the transformation of aragonite to calcite takes place by the dissolution of aragonite and precipitation of calcite in the presence of a hydrothermal phase, with the presence of such a fluid phase being critical for such a transformation. The veins display a network of vertical fractures and elongated pores between the vertical fibers (Figs. 3F and 3G). Although this aspect of the process has not been quantified, it is worth noting that this could accommodate the CO_2 bubble transport through the vein. From microstructural observations, growth increments cannot really be separated. Crystallization is more or less continuous over a duration of about one millennium, even if some heterogeneities of growth are seen, such as fan-shaped fibers growing from the same horizontal location or a horizontal alignment of fractures and pores. Horizontal stylolites (Fig. 3H) could be linked to dissolution of the fibers after their growth, as predicted when mineral growth is faster than the fracture opening (Bons, 2001) or when mineral growth increases stress in its surrounding volume (Merino et al., 2006).

In conclusion, in order to explain the results obtained from U-Th geochronological dating, which showed that horizontal travertine veins grow from top to bottom, uplifting the rock above them, it is suggested that such a vein growth process is driven by the carbonate crystallization force triggered by CO_2 degassing at 1–10 m depth. This mechanism of vein growth is widespread, as it has produced up to half of the total volume of travertine mounds along the Little Grand Wash and Salt Wash faults in Utah. It could be found in other travertines in the world. This study also shows that great care must be taken when interpreting travertine data from samples removed from drill holes, for paleoclimatic or paleomagnetic records (Andrews, 2006), because the ages of successive layers are not necessarily continuous from bottom to top in stratigraphic order. Finally, these veins also develop in the sandstone basement away from the travertine but always at limited distance from the fault that probably acts as a transitory flow path at regional scale. This may happen in other geological contexts where CO_2 degassing could drive mineral precipitation from carbonate-rich fluid flowing from depth along active faults.

ACKNOWLEDGMENTS

We thank N. Kampman and two anonymous reviewers for their comments, which significantly improved the manuscript.

REFERENCES CITED

Andrews, J.E., 2006, Paleoclimatic records from stable isotopes in riverine tufas: Earth-Science Reviews, v. 75, p. 85–104, doi:10.1016/j.earscirev.2005.08.002.

Assayag, N., Bickle, M., Kampman, N., and Becker, J., 2009, Carbon isotopic constraints on CO_2 degassing in cold-water geysers, Green River, Utah: Energy Procedia, v. 1, p. 2361–2366, doi:10.1016/j.egypro.2009.01.307.

Bons, P.D., 2001, Development of crystal morphology during unitaxial growth in a progressively widening vein: I. The numerical model: Journal of Structural Geology, v. 23, p. 865–872, doi:10.1016/S0191-8141(00)00159-0.

Deschamps, P., Durand, N., Bard, E., Hamelin, B., Camoin, G., Thomas, A.L., Henderson, G.M., Okuno, J., and Yokoyama, Y., 2012, Ice sheet collapse and sea-level rise at the Bølling warming 14,600 yr ago: Nature, v. 483, p. 559–564, doi:10.1038/nature10902.

Dockrill, B., 2006, Understanding leakage from a fault-sealed CO_2 reservoir in east-central Utah: A natural analogue applicable to CO_2 storage [Ph.D. thesis]: Dublin, Trinity College, 165 p.

Dockrill, B., and Shipton, Z.K., 2010, Structural controls on leakage from a natural CO_2 geologic storage site: Central Utah, USA: Journal of Structural Geology, v. 32, p. 1768–1782, doi:10.1016/j.jsg.2010.01.007.

Faccenna, C., Soligo, M., Billi, A., De Filippis, L., Funiciello, R., Rossetti, C., and Tuccimei, P., 2008, Late Pleistocene depositional cycle of the Lapis Tiburtinus travertines (Tivali, Central Italy): Possible influence of climate and fault activity: Global and Planetary Change, v. 63, p. 299–308, doi:10.1016/j.gloplacha.2008.06.006.

Fletcher, R.C., and Merino, E., 2001, Mineral growth in rocks: Kinetic-rheological models of replacement, vein formation, and syntectonic crystallization: Geochimica et Cosmochimica Acta, v. 65, p. 3733–3748, doi:10.1016/S0016-7037(01)00726-8.

Frery, E., 2012, Episodic circulation of reactive fluids along faults: From travertine- to basin-scale on the Colorado Plateau natural example (USA) [Ph.D. thesis]: University of Grenoble 1, University of Leuven, 247 p.

Hancock, P.L., Chalmers, R.M.L., Altunel, E., and Cakir, Z., 1999, Travitonics: Using travertines in active fault studies: Journal of Structural Geology, v. 21, p. 903–916, doi:10.1016/S0191-8141(99)00061-9.

Heath, J., 2004, Hydrogeochemical characterization of leaking carbon dioxide–charged faults zones in east-central Utah [M.S. thesis]: Logan, Utah, Utah State University, 103 p.

Hilgers, C., and Urai, J.L., 2005, On the arrangement of solid inclusions in fibrous veins and the role of the crack-seal mechanism: Journal of Structural Geology, v. 27, p. 481–494, doi:10.1016/j.jsg.2004.10.012.

Kampman, N., Bricke, M., Assayag, N., and Chapman, H.J., 2009, Feldspar dissolution kinetics and Gibbs free energy dependence in the CO_2-enriched groundwater system, Green River, Utah: Earth and Planetary Science Letters, v. 284, p. 473–488, doi:10.1016/j.epsl.2009.05.013.

Kampman, N., Burnside, N.M., Bickle, M., Shipton, Z.K., Ellam, R.M., and Chapman, H.J., 2010, Coupled CO_2-leakage and in situ fluid-mineral reactions in a natural CO_2 reservoir, Green River, Utah: Geochimica et Cosmochimica Acta, v. 74, p. A492.

Kampman, N., Burnside, N.M., Shipton, Z.K., Chapman, H.J., Nicholl, J.A., Ellam, R.M., and Bickle, M.J., 2012, Pulses of carbon dioxide emissions from intracrustal faults following climatic warming: Nature Geoscience, v. 5, p. 352–358, doi:10.1038/ngeo1451.

Merino, E., Canals, A., and Fletcher, R.C., 2006, Genesis of self-organized zebra textures in burial dolomites: Displacive veins, induced stress, and dolomitization: Geologica Acta, v. 4, p. 383–393.

Noiriel, C., Renard, F., Doan, M.L., and Gratier, J.P., 2010, Intense fracturing and fracture sealing induced by mineral growth in porous rocks: Chemical Geology, v. 269, p. 197–209, doi:10.1016/j.chemgeo.2009.09.018.

Oldenburg, C.M., and Lewicki, J.L., 2006, On leakage and seepage of CO_2 from geologic storage sites into surface water: Environmental Geology, v. 50, p. 691–705, doi:10.1007/s00254-006-0242-0.

Or, D., and Tuller, M., 2002, Cavitation during desaturation of porous media under tension: Water Resources Research, v. 38, p. 1061, doi:10.1029/2001WR000282.

Pentecost, A., 2005, Travertine: Berlin, Heidelberg, Springer, 453 p.

Perdikouri, C., Kasioptas, A., Putnis, C.V., and Putnis, A., 2008, The effect of fluid composition on the mechanism of the aragonite to calcite transition: Mineralogical Magazine, v. 72, p. 111–114, doi:10.1180/minmag.2008.072.1.111.

Shipton, Z.K., Evans, J.P., Kirschner, D., Kolesar, P.T., Williams, A.P., and Heath, J.E., 2004, Analysis of CO_2 leakage through "low-permeability" fault from natural reservoirs in the Colorado Plateau, southern Utah, *in* Baines, S.G., and Worden, R.H., eds., Geological storage of carbon dioxide: The Geological Society of London Special Publication 233, p. 43–58.

Steiger, M., 2005, Crystal growth in porous materials—I: The crystallization pressure of large crystals: Journal of Crystal Growth, v. 282, p. 455–469, doi:10.1016/j.jcrysgro.2005.05.007.

Style, R.W., Peppin, S.S.L., Cocks, A.C.F., and Wettlaufer, J.S., 2011, Ice-lens formation and geometrical supercooling in soils and other colloidal materials: Physical Review E, v. 84, 041402, doi:10.1103/PhysRevE.84.041402.

Taber, S., 1916, The growth of crystals under external pressure: American Journal of Science, v. 41, p. 532–556, doi:10.2475/ajs.s4-41.246.532.

Uysal, I.T., Feng, Y., Zhao, J.X., Altunel, E., Weatherley, D., Karabacak, V., Cengiz, O., Golding, S.D., Lawrence, M.G., and Collerson, K.D., 2007, U-series dating and geochemical tracing of late Quaternary travertine in co-seismic fissures: Earth and Planetary Science Letters, v. 257, p. 450–462, doi:10.1016/j.epsl.2007.03.004.

Weyl, P.K., 1959, Pressure solution and the force of crystallization: A phenomenological theory: Journal of Geophysical Research, v. 64, p. 2001–2025, doi:10.1029/JZ064i011p02001.

Wiltschko, D.V., and Morse, J.W., 2001, Crystallization pressure versus "crack seal" as the mechanism for banded veins: Geology, v. 29, p. 79–82, doi:10.1130/0091-7613(2001)029<0079:CPVCSA>2.0.CO;2.

Manuscript received 10 February 2012
Revised manuscript received 30 April 2012
Manuscript accepted 7 May 2012

Printed in USA